

Fine tuning the surface acidity of titanate nanostructures

D. Madarász · I. Szentí · L. Nagy · A. Sápi ·
Á. Kukovecz · Z. Kónya

Received: 5 December 2012 / Accepted: 31 January 2013 / Published online: 9 February 2013
© Springer Science+Business Media New York 2013

Abstract The effect of protonation on the surface acidic properties of titanate nanowires (TiONWs) was investigated. Nanowires were synthesized by the alkali hydrothermal method which resulted in one dimensional nanostructures of large external surface area and well-defined lamellar interlayer structure. The Na^+/H^+ ratio in the structure can be tuned by ion-exchange. Our aim was to characterize the morphology of the as-synthesized nanostructures by HRTEM and SEM measurements and assess their surface acidity using in situ infrared spectroscopic measurements and temperature programmed desorption. It was found that the numbers of Lewis and Brönsted acidic sites in the Na-form and the H-form of the TiONWs is different. The ratio and the nature of acidic sites can be tuned by the ion exchange process. The wire-like morphology and the tunable acidity are features of titanate nanowires that may render them a promising material in various heterogeneous catalytic applications.

Keywords Titanate nanowires · Surface acidity · Pyridine adsorption · Solid acids

1 Introduction

Titanate nanostructures like nanotubes and nanowires have attracted considerable attention from the scientific community because of their unique structure and properties. Many potential applications have emerged since Kasuga et al. (1998) reported first on an alkali hydrothermal method resulting in tubular titanate nanostructures. The material can be used as anode for lithium ion batteries or lithium storage devices (Li et al. 2005; Zhu et al. 2012), adsorbent for heavy metal ions removal from water (Yang et al. 2008, 2011), catalyst support (Hodos et al. 2005; Kukovecz et al. 2011; Toth et al. 2012) electrode of dye-sensitized solar cells (Ohsaki et al. 2005) humidity sensor (Zhang et al. 2008), mechanical reinforcement agent for polymers (Byrne et al. 2007) and as a starting material for one dimensional photocatalyst synthesis (Darányi et al. 2011; Hodos et al. 2004; Mor et al. 2005; Wu et al. 2011). The majority of reports published so far on one dimensional titanate nanostructure usage in the field of catalysis focused on photocatalytic applications for the decomposition of organic contaminants.

Surface constitution in general and surface acidic and basic properties in particular play key roles in heterogeneous catalytic reactions. Pyridine is a widely used probe molecule to assess the nature of surface acidic sites. The spectral analysis of adsorbed pyridine provides both qualitative and quantitative information about the surface acidity of solids. While the surface properties of isotropic anatase and rutile have been thoroughly investigated (Bezrodna et al. 2003; Martra 2000), reports on the acidity of tubular or wire-like titanate nanostructures are scarcely found in the literature. Toledo-Antonio et al. (2010) studied the morphology dependence of surface acidity in both tubular and particulate titanate materials. They have found

D. Madarász · I. Szentí · L. Nagy · A. Sápi · Á. Kukovecz ·
Z. Kónya
Department of Applied and Environmental Chemistry,
University of Szeged, Rerrich Béla tér 1, Szeged 6720, Hungary

Á. Kukovecz
MTA-SZTE “Lendület” Porous Nanocomposites Research
Group, Rerrich ter 1, Szeged 6720, Hungary

Z. Kónya (✉)
MTA-SZTE Reaction Kinetics and Surface Chemistry Research
Group, Rerrich ter 1, Szeged 6720, Hungary
e-mail: konya@chem.u-szeged.hu

that the morphology has a great effect on the ratio of physisorbed, H-bonded and coordinatively bonded pyridine.

Kitano et al. (2010) studied the surface acidity and catalytic activity of protonated titanate nanotubes by comparing them with conventional solid catalysts. They observed that ion-exchanged titanate nanotubes possess both Lewis and Brønsted type acidic sites while titanium-dioxide exhibits Lewis acidity only.

In this study we determined the surface acidic properties of titanate nanowires from the spectral analysis of adsorbed pyridine to examine the possibilities of their usage in heterogeneous catalysis.

2 Experimental

2.1 Sample preparation

Titanate nanowires were synthesized by an alkali hydrothermal method as described by Horváth et al. (2007). In a typical synthesis, 50 g of anatase TiO_2 powder purchased from Fluka was mixed with 1 L of 10 M NaOH (Sigma-Aldrich) solution. The suspension was filled into a Teflon lined stainless steel autoclave. The vessel was put into a furnace for 24 h at 190 °C. The autoclave was rotated around its shorter axis at a speed of 28 rpm. After 24 h the product slurry was filtered and washed with distilled water to neutral pH. The nanowires were dried in air at 70 °C for 24 h.

A series of protonated samples were prepared by ion-exchange to produce H-form or partially protonated nanowires. Suspensions were made of 1 g pristine titanate nanowires and 100 mL HCl solution in six different concentrations (0.01, 0.02, 0.03, 0.04, 0.06 and 0.1 M). After 12 h of intense stirring the suspensions was filtered and washed with distilled water until chloride ions were undetectable in the filtrate. The absence of Cl^- was verified by AgNO_3 probing. The nanowires were dried in air at 70 °C for 24 h.

2.2 Characterization

The morphology of the as-synthesized Na- and H-form titanate nanowires was characterized by a TECNAI G² 20×-Twin High-resolution transmission electron microscope (TEM) working at an accelerating voltage of 200 kV. Samples for TEM measurements were drop-casted onto carbon coated copper grids from acetone suspension.

Surface morphology characterization and semi-quantitative chemical analysis of the nanomaterials were

performed in a HITACHI S-4700 Type II cold field emission scanning electron microscope (SEM) operated at 20 kV accelerating voltage, by using the integrated Röntec QX2 EDS detector. In order to monitor the ion-exchange process, the quantitative analysis of the sodium content was necessary. The Na/Ti atomic ratio was evaluated from the sodium and titanium signals. Since the accuracy of EDS depends on many factors like the orientation, density of materials, etc., and the EDS result may not be accurate if the chemical composition of specimens is complex or the concentration of a target atom is too low, ten randomly chosen points were analyzed and an average value was calculated. The EDS probe size was about $10 \times 10 \mu\text{m}$ and the sampling depth of the analysis was around $1 \mu\text{m}$. The accuracy of EDX analysis was approximately $\pm 0.5 \text{ vol.}\%$.

The crystallographic properties were studied using a Rigaku Miniflex II powder X-ray diffractometer (XRD) equipped with a $\text{Cu K}\alpha$ radiation source ($\lambda = 0.15418 \text{ nm}$) by applying a scanning rate of 4° min^{-1} in the 2θ range of 5° – 80° .

The specific surface area was determined from N_2 adsorption analysis performed in a Quantachrome NOVA 3,000e surface area and pore size analyzer. Samples were degassed for 1 h at 200 °C in dynamic vacuum before the measurements.

Thermogravimetric analyses were carried out in a Setaram Labsys instrument. Samples (10 mg) were heated from 25 to 600 °C in nitrogen atmosphere at $10^\circ \text{C min}^{-1}$ heating rate.

The strength of acidic sites was determined by the NH_3 -TPD technique using a Belcat A instrument. The heating rate was set at $10^\circ \text{C min}^{-1}$ from 25 to 600 °C in helium atmosphere. The samples were pretreated for 1 h at 80 °C in helium flow.

Infrared absorption spectra were recorded on a Bruker Vertex 70 FT-IR instrument in the 400 – $4,000 \text{ cm}^{-1}$ range at a spectral resolution of 4 cm^{-1} . Self-supporting pellets of TiONW samples were prepared for the in situ infrared measurements by pressing 6 mg of TiONW into a 12 mm diameter pellet using a pressure of 25 MPa. The pellets were moved into a custom built adsorption chamber designed for infrared measurement and degassed at 80 °C temperature in vacuum for 1 h. Pyridine adsorption was then performed at room temperature at 133 Pa for 30 min followed by an additional 30 min evacuation process to remove excess pyridine adsorbed on non-acidic sites.

In-situ infrared spectroscopic measurements were carried out after pre-treating, after the pyridine adsorption phase and after evacuation. Spectra shown here were obtained by subtracting the pre-treated TiONW spectra from those recorded after pyridine adsorption and subsequent evacuation.

3 Results and discussion

3.1 Structure and morphology

Titanate nanowires were obtained by the alkali hydrothermal conversion of anatase TiO_2 powder. The as-synthesized nanowires are wire-like structures measuring 80–100 nm in diameter and 1–5 μm in length. Nanowires are known to be the thermodynamically most stable form of sodium trititanate under the applied hydrothermal synthesis conditions (Horváth et al. 2007).

Increasing the hydrochloric acid concentration in the ion exchange treatment decreased the sodium contents of the TiONWs as indicated by Fig. 1. The equilibrium composition is gradually shifted from the starting $\text{Na}_2\text{Ti}_3\text{O}_7$ compound through partially protonated $\text{Na}_{(2-x)}\text{H}_x\text{Ti}_3\text{O}_7$ stages until the final $\text{H}_2\text{Ti}_3\text{O}_7$ form is reached.

Characteristic XRD patterns of pristine (Na-form) and the fully protonated (H-form) TiONWs are shown in Fig. 2. The as-synthesized sample (Na-form) exhibited broad peaks of low intensity, which are quite difficult to index, but the profile could be referred to as reflections (around 10, 25, 28 and 49°) of sodium trititanate $\text{Na}_2\text{Ti}_3\text{O}_7$ (JCPDS no. 31-1329). Other researchers have proposed different crystalline phases for the as-synthesized samples, for example lepidocrocite titanates (Sasaki et al. 1997; Ma et al. 2004) or divalent salt titanate ($\text{Na}_2\text{Ti}_2\text{O}_5 \cdot \text{H}_2\text{O}$) (Tsai and Teng 2006), etc. The crystalline structure of these samples is metastable and contains water and sodium in its matrix, therefore, the exact formulation depends on the synthesis condition and the volume of the sealed or filled factor (Poudel et al. 2005). After the ion-exchange process, the most intense peak of the titanate structure [the reflection at $2\theta \approx 10^\circ$ assigned to the (0 0 1) crystal plane]

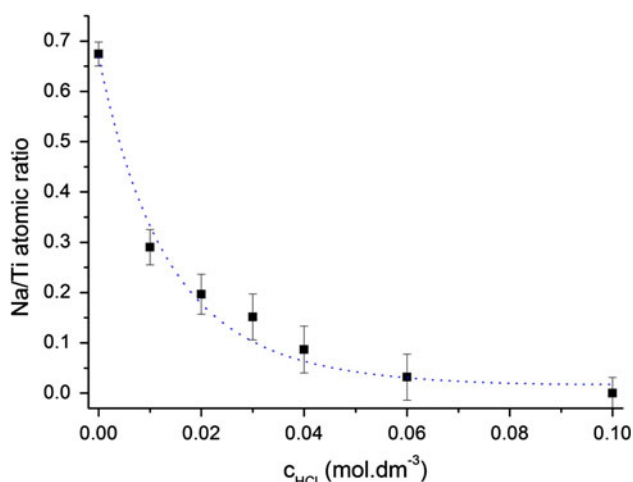


Fig. 1 Na/Ti ratio in ion exchanged TiONWs (calculated from EDX data)

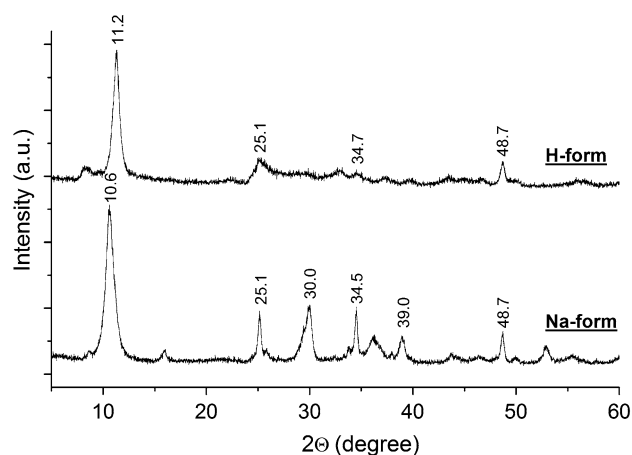


Fig. 2 XRD patterns of Na- and H-form TiONWs

shifts to a higher angle. According to the crystal structure reported by Peng et al. (2008), this low angle peak represents the crystal plane spacing between two Ti–O layers, thus the Ti–O interlayer spaces appear to have been narrowed as a result of the replacement of the interlayer Na^+ ions by H^+ (or rather H_3O^+) ions (Zhao et al. 2011). Since there is a Na–O layer between the Ti–O layers which tends to be affected by post-treatments, such as washing, ion-exchange, or drying, the identification of the structure of acid-washed product as layered hydrogen titanate $\text{H}_2\text{Ti}_3\text{O}_7 \cdot n\text{H}_2\text{O}$ (JCPDS no. 36-0654) is obvious.

The TEM measurements depicted in Fig. 3. confirmed that the nanowire morphology was unaffected by the ion exchange process. The specific surface area of the Na-form and H-form TiONWs was 28.7 and 35.3 $\text{m}^2 \text{g}^{-1}$, respectively. This difference can be explained by the molar weight difference between the two forms adequately ($\text{Na}_2\text{Ti}_3\text{O}_7$ to $\text{H}_2\text{Ti}_3\text{O}_7$), therefore, the specific surface area measurement verifies the preservation of the one dimensional nanowire morphology.

3.2 Thermogravimetry

Knowing the thermal stability of one dimensional titanate nanostructures is very important, because several potential applications and/or modifications require higher temperatures. The thermogravimetric characterization of the thermal behavior of titanate nanowires is depicted in Fig. 4. There are two important weight loss steps in both the Na- and the H-form. The first one takes place between 50–120 $^\circ\text{C}$ and it is related to the release of adsorbed water. In pristine Na-form nanowires the second step starts at 110 $^\circ\text{C}$ and ends at 320 $^\circ\text{C}$ as wires loose structural water transforming from trititanate into a mixed titanate form of $\beta\text{-TiO}_2$ and sodium-hexatitanate ($\text{Na}_2\text{Ti}_6\text{O}_{13}$). In case of H-form wires the

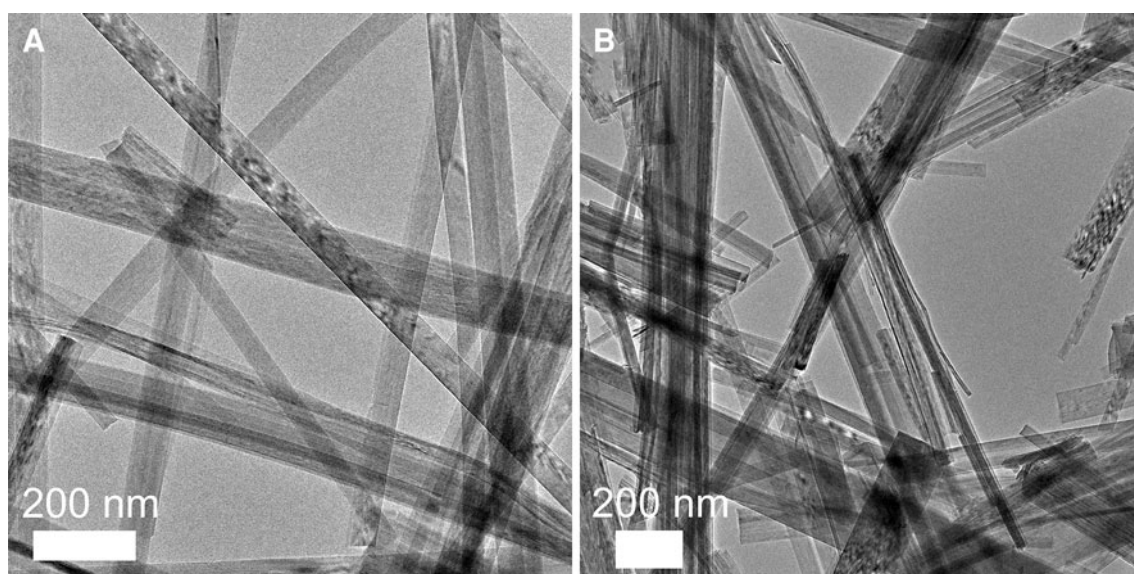


Fig. 3 TEM image of Na- (a) and H-form (b) TiONWs

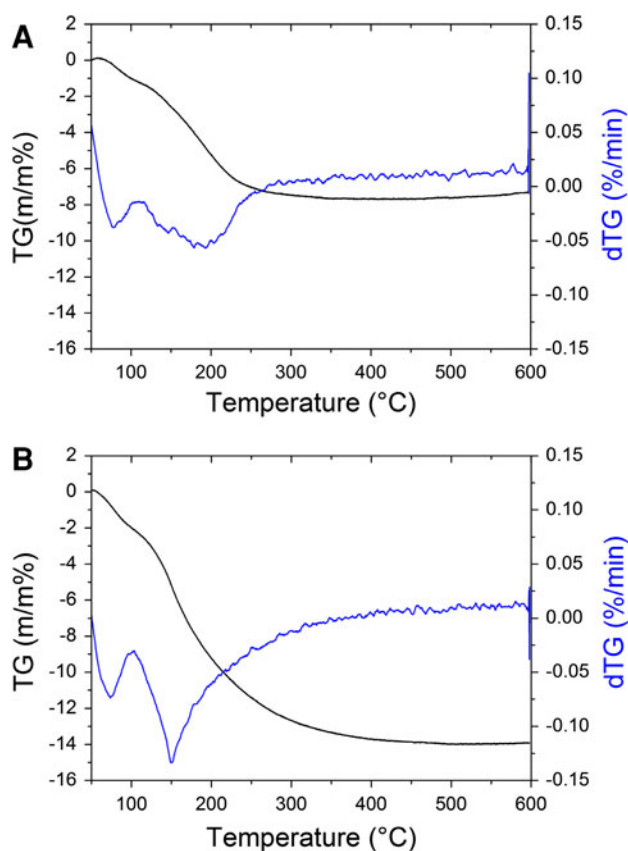


Fig. 4 TG and dTG curve of Na- (a) and H-form (b) TiONWs

second weight loss step ends at a higher temperature (450 °C) and the weight loss is larger than in the case of Na-form TiONW (14 versus 8 m/m %). The reason for this that structural oxygen is removed from the H-form nanowires as they transform into anatase: $\text{H}_2\text{Ti}_3\text{O}_7 \rightarrow 3\text{TiO}_2 + \text{H}_2\text{O}$

3.3 Infrared spectroscopy

The analysis of the fine structure of the infrared bands of adsorbed pyridine is a well-established method for assessing zeolite acidity. Typical pyridine bands observed in the $1,400\text{--}1,650\text{ cm}^{-1}$ spectral range indicate the presence of pyridine adsorbed on Lewis and Brönsted acidic sites as well as physisorbed pyridine. Bands at $1,443$ and $1,606\text{ cm}^{-1}$ can be assigned to pyridine adsorbed on strong Lewis type acid sites (Ertl et al. 1997; Parry 1963). Bands at $1,575$ and $1,594\text{ cm}^{-1}$ are assigned to physisorbed, hydrogen bonded pyridine (Cook 1961; Parry 1963). The presence of the $1,488\text{ cm}^{-1}$ band indicates that pyridine interacts with both types of active centers (Parry 1963). Finally, the broad band at $1,549\text{ cm}^{-1}$ with the additional band at $1,641\text{ cm}^{-1}$ evidence the presence of Brönsted acid sites (Kitano et al. 2010; Parry 1963). We hypothesized that the same technique is applicable to one dimensional titanate nanostructures because of the similarity of their negatively charged, ion-exchange capable framework. In Fig. 5 the spectra of pyridine adsorbed on both Na-form and H-form titanate nanowires are presented. It is remarkable to note that the same band assignment valid for zeolites can be used for titanate nanowires as well (Gonzalez Pena et al. 2011; Kónya et al. 1996; Halász et al. 1996). Therefore, TiONW pyridine adsorption spectra can be evaluated by using the analogy of the Na-faujasite/H-faujasite zeolite pair. Na-form TiONWs exhibit two types of Lewis acid sites originating from Na^+ ions and coordinatively unsaturated framework Ti^{4+} ion related oxygen vacancies. The sodium ion is the stronger one as indicated by the presence of the $\sim 1,625\text{ cm}^{-1}$ band, which is known to

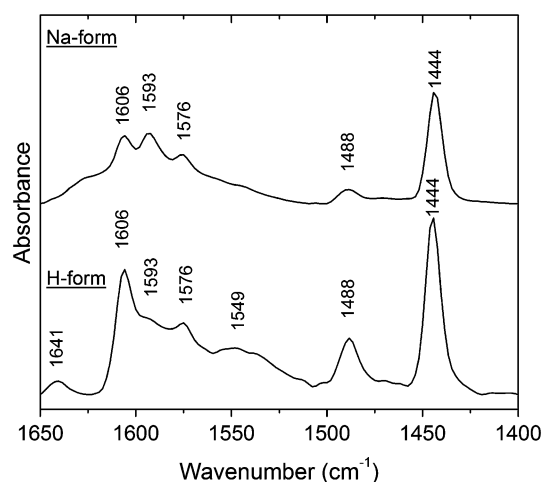


Fig. 5 FTIR spectra of adsorbed pyridine on Na- and H-form TiONWs

measure the strength of Lewis acid sites (Busca 1998). This band disappears after protonation, whereas the $1,606\text{ cm}^{-1}$ band assigned to pyridine adsorbed on framework Lewis acid sites is still observable. Interestingly, Na-form TiONWs exhibit Brönsted acidity as well (indicated by the $1,557\text{ cm}^{-1}$ band) which is related to the formation of mobile protons by the interaction of the titanate framework and residual water in the structure. New features in the H-form pyridine spectrum appearing at $1,549$ and $1,641\text{ cm}^{-1}$ as well as the increased intensity of the band at $1,488\text{ cm}^{-1}$ indicate the formation of Brönsted acid sites upon the protonation of TiONWs. Moreover, the high intensity band observable at $1,444\text{ cm}^{-1}$ and the significantly increased band at $1,606\text{ cm}^{-1}$ evidence that the amount of Lewis type acidic sites was increased as well. The presence of this type of acidity in trititanates agrees well with the general structural model of titanium oxide derivatives consisting of octahedral TiO_6 building blocks (Horváth et al. 2007; Kukovecz et al. 2005). In fact, Lewis acidity was reportedly observed in TiO_2 species earlier by several authors (Toledo-Antonio et al. 2010). The hydrochloric acid treatment increases the number of vacancies and simultaneously generates Brönsted acid sites by protonating the titanate nanowires.

3.4 NH_3 -TPD

On the TPD curve of Na-form nanowires the TDC signal has only one maximum in the temperature range of $100\text{--}300^\circ\text{C}$ with a shoulder at around 260°C and a maximum at 178°C (Fig. 6). This agrees well with the FT-IR results and confirms that Na-form titanate nanowires

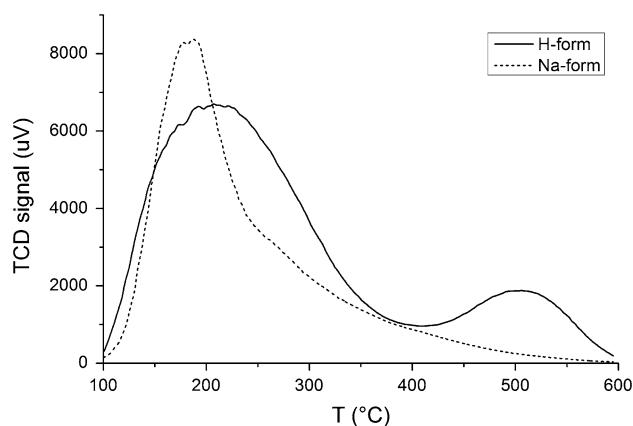


Fig. 6 NH_3 -TPD curves of Na- and H-form TiONWs

can interact with basic probe molecules as Lewis acids. However, it should be noted that the low temperature loss of physisorbed pyridine and structural water can also contribute to the overall TDC signal. The ammonia TPD signal of H-form TiONWs is characteristically different from that of the Na-form material. The first desorption peak is upshifted to 207°C indicating that Lewis acid sites are stronger in the protonated nanowires. Moreover, a second peak is observable in the TPD signal at 504°C which can be assigned to the desorption of pyridine bound to Brönsted acid sites. The thermal stability of these acid sites in protonated titanate nanowires is quite remarkable because the material is known to experience crystal phase transitions in this temperature range.

4 Conclusion

The surface acidic properties of titanate nanowires synthesized by the alkali hydrothermal method were studied. We conclude that Na-form TiONWs exhibit Lewis acidity only, whereas protonated H-form nanowires contain both Lewis and Brönsted acid sites. We demonstrated that the Na⁺/H⁺ ratio can be tuned by controlling the ion exchange procedure. The protonation of titanate nanowires is a suitable process for increasing the strength of Lewis acid sites and generating new Brönsted acid centers while preserving the layered structure and one-dimensional morphology of the nanowires. These findings may facilitate the usage of titanate nanowires in heterogeneous catalytic applications involving acid–base type reactions.

Acknowledgments The financial support of the TÁMOP-4.2.2.A-11/1/KONV-2012-0047 and TÁMOP-4.2.2.A-11/1/KONV-2012-0060 projects and the EC FP7 INCO “NAPEP” network is acknowledged.

References

- Bezrodna, T., Puchkovska, G., Shimanovska, V., Chashechnikova, I., Khalyavka, T., Baran, J.: Pyridine–TiO₂ surface interaction as a probe for surface active centers analysis. *Appl. Surf. Sci.* **214**, 222–231 (2003)
- Busca, G.: Spectroscopic characterization of the acid properties of metal oxide catalysts. *Catal. Today* **41**, 191–206 (1998)
- Byrne, M.T., McCarthy, J.E., Bent, M., Blake, R., Gunko, Y.K., Horvath, E., Konya, Z., Kukovecz, A., Kiricsi, I., Coleman, J.N.: Chemical functionalisation of titania nanotubes and their utilisation for the fabrication of reinforced polystyrene composites. *J. Mater. Chem.* **17**, 2351–2358 (2007)
- Cook, D.: Vibrational spectra of pyridinium salts. *Can. J. Chem.* **39**, 2009–2024 (1961)
- Darányi, M., Csesznok, T., Kukovecz, A., Konya, Z., Kiricsi, I., Ajayan, P.M., Vajtai, R.: Layer-by-layer assembly of TiO₂ nanowire/carbon nanotube films and characterization of their photocatalytic activity. *Nanotechnology* **22**, 195701 (2011)
- Ertl, G., Knötzing, H., Weitkamp, J.: *Handbook of Heterogeneous Catalysis*. VCH Verlagsgesellschaft mbH, Weinheim (1997)
- Gonzalez Pena, L.F., Sad, M.E., Padro, C.L., Apesteguia, C.R.: Study of the alkylation of phenol with methanol on Zn(H)-exchanged NaY zeolites. *Catal. Lett.* **141**, 939–947 (2011)
- Halász, J., Kónya, Z., Fudala, A., Béres, A., Kiricsi, I.: Indium and gallium containing ZSM-5 zeolites: acidity and catalytic activity in propane transformation. *Catal. Today* **31**, 293–304 (1996)
- Hodos, M., Horvath, E., Haspel, H., Kukovecz, A., Konya, Z., Kiricsi, I.: Photo sensitization of ion-exchangeable titanate nanotubes by CdS nanoparticles. *Chem. Phys. Lett.* **399**, 512–515 (2004)
- Hodos, M., Kónya, Z., Kiricsi, I.: Catalysis by pre-prepared platinum nanoparticles supported on trititanate nanotubes. *React. Kinet. Catal. Lett.* **84**, 341–350 (2005)
- Horváth, E., Kukovecz, A., Konya, Z., Kiricsi, I.: Hydrothermal conversion of self-assembled titanate nanotubes into nanowires in a revolving autoclave. *Chem. Mater.* **19**, 927–931 (2007)
- Kasuga, T., Hiramatsu, M., Hoson, A., Sekino, T., Nihara, K.: Formation of titanium oxide nanotubes. *Langmuir* **14**, 3160–3163 (1998)
- Kitano, M., Nakajima, K., Kondo, J.N., Hayashi, S., Hara, M.: Protonated titanate nanotubes as solid acid catalyst. *J. Am. Chem. Soc.* **132**, 6622–6623 (2010)
- Kónya, Z., Hannus, I., Kiricsi, I.: Infrared spectroscopic study of adsorption and reactions of methyl chloride on acidic, neutral and basic zeolites. *Appl. Catal. B Environ.* **8**, 391–404 (1996)
- Kukovecz, A., Hodos, M., Horvath, E., Radnóczy, G., Konya, Z., Kiricsi, I.: Oriented crystal growth model explains the formation of titania nanotubes. *J. Phys. Chem. B* **109**, 17781–17783 (2005)
- Kukovecz, A., Potari, G., Oszko, A., Konya, Z., Erdohelyi, A., Kiss, J.: Probing the interaction of Au, Rh and bimetallic Au–Rh clusters with the TiO₂ nanowire and nanotube support. *Surf. Sci.* **605**, 1048–1055 (2011)
- Li, J.R., Tang, Z.L., Zhang, Z.T.: Layered hydrogen titanate nanowires with novel lithium intercalation properties. *Chem. Mater.* **17**, 5848–5855 (2005)
- Ma, R., Bando, Y., Sasaki, T.: Directly rolling nanosheets into nanotubes. *J. Phys. Chem. B* **108**, 2115–2119 (2004)
- Martra, G.: Lewis acid and base sites at the surface of microcrystalline TiO₂ anatase: relationships between surface morphology and chemical behavior. *Appl. Catal. A Gen.* **200**, 275–285 (2000)
- Mor, G.K., Shankar, K., Paulose, M., Varghese, O.K., Grimes, C.A.: Enhanced photocleavage of water using titania nanotube arrays. *Nano Lett.* **5**, 191–195 (2005)
- Ohsaki, Y., Masaki, N., Kitamura, T., Wada, Y., Okamoto, T., Sekino, T., Niihara, K., Yanagida, S.: Dye-sensitized TiO₂ nanotube solar cells: fabrication and electronic characterization. *Phys. Chem. Chem. Phys.* **7**, 4157–4163 (2005)
- Parry, E.P.: An infrared study of pyridine adsorbed on acidic solids. Characterization of surface acidity. *J. Catal.* **2**, 371–379 (1963)
- Peng, C.W., Richard-Plouet, M., Ke, T.Y., Lee, C.Y., Chiu, H.T., Marhic, C., Puzenat, E., Lemoigno, F., Brohan, L.: Chimie douce route to sodium hydroxo titanate nanowires with modulated structure and conversion to highly photoactive titanium dioxides. *Chem. Mater.* **20**, 7228–7236 (2008)
- Poudel, B., Wang, W., Dames, C., Huang, J., Kunwar, S., Wang, D., Barnerjee, D., Chen, G., Ren, Z.: Formation of crystallized titania nanotubes and their transformation into nanowires. *Nanotechnology* **16**, 1935 (2005)
- Sasaki, T., Ma, R., Nakano, S., Yamauchi, S., Watanabe, M.: Fabrication of titanium dioxide thin flakes and their porous aggregate. *Chem. Mater.* **9**, 602–608 (1997)
- Tsai, C., Teng, H.: Structural features of nanotubes synthesized from NaOH treatment on TiO₂ with different post-treatments. *Chem. Mater.* **18**, 367–373 (2006)
- Toledo-Antonio, J.A., Cortes-Jacome, M.A., Navarrete, J., Angeles-Chavez, C., Lopez-Salinas, E., Rendon-Rivera, A.: Morphology induced CO, pyridine and lutidine adsorption sites on TiO₂: Nanoparticles, nanotubes and nanofibers. *Catal. Today* **155**, 247–254 (2010)
- Toth, M., Kiss, J., Oszko, A., Potari, G., Laszlo, B., Erdohelyi, A.: Hydrogenation of carbon dioxide on Rh, Au and Au–Rh bimetallic clusters supported on titanate nanotubes, nanowires and TiO₂. *Top. Catal.* **55**, 747–756 (2012)
- Wu, M.C., Hiltunen, J., Sapi, A., Avila, A., Larsson, W., Liao, H.C., Huuhtanen, M., Toth, G., Shchukarev, A., Laufer, N., Kukovecz, A., Konya, Z., Mikkola, J.P., Keiski, R., Su, W.F., Chen, Y.F., Jantunen, H., Ajayan, P.M., Vajtai, R., Kordas, K.: Nitrogen-doped anatase nanofibers decorated with noble metal nanoparticles for photocatalytic production of hydrogen. *ACS Nano* **5**, 5025–5030 (2011)
- Yang, D.J., Sarina, S., Zhu, H.Y., Liu, H.W., Zheng, Z.F., Xie, M.X., Smith, S.V., Komarneni, S.: Capture of radioactive cesium and iodide ions from water by using titanate nanofibers and nanotubes. *Angew. Chem. Int. Ed.* **50**, 10594–10598 (2011)
- Yang, D.J., Zheng, Z.F., Zhu, H.Y., Liu, H.W., Gao, X.P.: Titanate nanofibers as intelligent absorbents for the removal of radioactive ions from water. *Adv. Mater.* **20**, 2777–2781 (2008)
- Zhang, Y.Y., Fu, W.Y., Yang, H.B., Li, M.H., Li, Y.X., Zhao, W.Y., Sun, P., Yuan, M.X., Ma, D., Liu, B.B., Zou, G.T.: A novel humidity sensor based on Na₂Ti₃O₇ nanowires with rapid response-recovery. *Sens. Actuators B Chem.* **135**, 317–321 (2008)
- Zhao, B., Chen, F., Liu, H., Zhang, J.: Mesoporous TiO₂-B nanowires synthesized from tetrabutyl titanate. *J. Phys. Chem. Solids* **72**, 201–206 (2011)
- Zhu, G.N., Wang, Y.G., Xia, Y.Y.: Ti-based compounds as anode materials for Li-ion batteries. *Energy Environ. Sci.* **5**, 6652–6667 (2012)